Infrared observation of transverse and longitudinal polar optical modes of semiconductor films: Normal and oblique incidence

M. Dean Sciacca, A. J. Mayur, Eunsoon Oh, A. K. Ramdas, and S. Rodriguez
Department of Physics, Purdue University, West Lafayette, Indiana 47907-1396

J. K. Furdyna
Department of Physics, University of Notre Dame, Notre Dame, Indiana 46556

M. R. Melloch
School of Electrical Engineering, Purdue University, West Lafayette, Indiana 47907-1390

C. P. Beetz and W. S. Yoo
Advanced Technology Materials, Inc., Danbury, Connecticut 06810
(Received 24 October 1994)

The observation of the zone-center transverse optic (TO) and longitudinal optic (LO) phonons of a polar semiconductor crystal as transmission minima in its infrared spectrum, when measured with radiation obliquely incident on a thin film of the crystal, i.e., the Berreman effect, is applied to a diverse group of II-VI and III-V epilayers and superlattices grown by molecular-beam epitaxy (MBE) as well as epilayers of SiC on a Si substrate and free-standing CdS films grown by chemical-vapor deposition (CVD). Whereas the TO phonon appears irrespective of the polarization of the incident radiation for both normal and oblique incidence, the LO phonon can be detected only in the latter with light polarized in the plane of incidence. The technique, successfully applied to tetrahedrally coordinated zinc-blende MnTe, accessible only with MBE growth on GaAs, has resulted in a direct observation of its TO and LO modes. Zinc-blende $Cd_{1-x}Mn_xSe$ grown on GaAs by MBE, similarly investigated, yields the frequencies of the CdSe-like and MnSe-like TO and LO modes as a function of x, including those for cubic CdSe ($x = 0$) and, by extrapolation to $x = 1$, for zinc-blende MnSe. In the II-VI/II-VI superlattices, confinement of the optical phonons has been observed. In free-standing CdS films with the wurtzite structure, their optic axis being in the plane of the film, the A_1(TO), E_1(TO), and E_1(LO) zone-center phonons have been directly observed. In a GaAs/AlAs/GaAs structure grown by MBE, the LO and TO modes of the submicrometer AlAs epilayer and the GaAs cap layer were observed with the Berreman technique, before and after removing the GaAs substrate, respectively. Finally, the Berreman effect of cubic SiC, grown on a Si substrate by CVD, illustrates the power of the technique in the context of a material of increasing technological importance.

I. INTRODUCTION

Nearly a century ago Rubens and Nichols discovered in alkali halides a band of total reflection in the infrared, the so-called reststrahlen band.[1] It is well known that it spans the region between the frequencies of the zone-center transverse optical (TO) and longitudinal optical (LO) phonons, i.e., between the pole and zero of the dielectric function corresponding to the zone-center infrared active lattice vibration.[2] In ionic crystals with the NaCl structure, or in tetrahedrally coordinated zinc-blende semiconductors, there is only one zone-center optical mode which in turn undergoes the characteristic LO-TO splitting, originating in the associated long wavelength polarization fields; in these crystals the zone-center TO and LO frequencies ω_{TO} and ω_{LO}, respectively, are related to the static (ϵ_0) and optical (ϵ_∞) dielectric constants by the Lyddane-Sachs-Teller (LST) relation $\omega_{LO}/\omega_{TO} = (\epsilon_0/\epsilon_\infty)^{1/2}$. (In the present paper, since we deal only with zone-center phonons, we omit this designation.) In uniaxial crystals with the wurtzite structure, there are infrared active optical modes, which are polarized either parallel to the optic axis or normal to it; thus two dielectric functions are required, one for each polarization, in order to analyze their reststrahlen spectrum. In biaxial crystals one has to analyze the reststrahlen phenomenon in the context of the three principal axes of the optical indicatrix, thus requiring three corresponding dielectric functions.

One can deduce ω_{TO} and ω_{LO} from the infrared reflectivity spectrum of a crystal by a curve-fitting procedure. For example, in an alkali halide or a zinc-blende crystal, the experimental reflectivity is compared with that theoretically deduced using a dielectric function containing ϵ_0, ϵ_∞, ω_{TO}, and γ (the damping coefficient) as adjustable parameters. While this procedure is useful, it is computer intensive. These drawbacks can be avoided if one could *directly* measure ω_{TO} and ω_{LO}. The TO phonon frequency was first directly measured by Barnes

and Czerny[3] in thin alkali halide films using transmission spectroscopy at *normal* incidence.

An alternate method for measuring ω_{TO} and ω_{LO} is Raman scattering. While in the zinc-blende structure the polar modes are Raman active, in the alkali halides, which possess center of inversion symmetry, the rule of mutual exclusion prevents their observation in the first-order Raman effect thus making infrared absorption the only available direct technique; but then one cannot observe the LO mode. Raman scattering has been extensively employed to determine the phonon energies in the zinc-blende semiconductors.[4] The ease of observation of the polar modes depends upon the resonant enhancement with an appropriate excitation laser frequency to match the band gap or the exciton energy. The selection rules for allowed transitions for any particular crystal structure can be determined by group theory. In the case of zinc-blende crystals, the TO is not allowed in Raman scattering in the [100] backscattering geometry. This is significant since a large number of III-V or II-VI thin films grown by molecular-beam epitaxy (MBE) have zinc-blende symmetry with [100] growth axis. Thus, for such films another technique for observing the TO is desirable.

All the above drawbacks can be overcome in a very simple and elegant manner by resorting to infrared transmission or reflection at *oblique incidence*, first predicted and verified by Berreman in thin LiF films on a collodion film.[5] He showed that for radiation at *oblique* incidence and with the electric vector polarized perpendicular to the plane of incidence there is only one transmission minimum at ω_{TO}, but for the electric vector polarized parallel to the plane of incidence, transmission minima are observed at both ω_{TO} and ω_{LO}. These experiments clearly demonstrate the ease of the technique, the only restriction being that the films must be significantly thinner than the wavelength of the electromagnetic radiation corresponding to that of the reststrahlen band, as is generally the case for MBE-grown epilayers and heterostructures. Indeed, access to high quality epilayers grown by MBE as well as by metal-organic chemical-vapor deposition and liquid-phase epitaxy provides an opportunity to discover and delineate the transverse and longitudinal optical phonons in all of the tetrahedrally coordinated III-V and II-VI semiconductors as well as the IV-VI semiconductors such as PbTe, which have the NaCl structure. In addition, novel materials such as zinc-blende MnTe and MnSe are now available, thanks to new nonequilibrium growth techniques. Following Berreman's original work, several other systems have been studied using the same technique. These include GaAs;[6] CaF_2, SrF_2, and BaF_2;[7] AgCl, AgBr, and AgI;[8] CuCl;[9] ZnSe and ZnTe;[10] and CdS.[11]

In this paper we present an account of the Berreman-technique-based experimental investigation of the LO and TO modes of MBE-grown zinc-blende II-VI and III-V semiconductors as well as SiC and CdS grown by chemical-vapor deposition (CVD).[12] The presentation includes the relevant electromagnetic theory of transmission and reflection of thin films and multilayer structures to provide the basis for the analysis of the experimental results.

II. EXPERIMENT

In the present investigation, based on the Berreman technique, infrared transmission measurements were performed on free-standing thin films as well as on a diverse group of epilayers and superlattices grown on substrates. Two epilayers unique by virtue of their structure are MBE-grown zinc-blende MnTe (~ 1 μm thick) and CdSe (~ 1 μm thick); we note that in bulk they exist in NiAs and wurtzite structures, respectively. Both are grown on GaAs substrates, but the MnTe epilayer has a 2-μm-thick ZnTe buffer. We also examined a number of zinc-blende $Zn_xCd_{1-x}Se$ epilayers and $Cd_xMn_{1-x}Se$ epilayers grown on GaAs substrates[13] by MBE as well as a ZnTe/CdSe superlattice on GaAs comprised of 25 periods of CdSe (45 Å) and ZnTe (90 Å). (It should be emphasized that in their bulk form, $Zn_xCd_{1-x}Se$ for $x \leq 0.6$ and $Cd_xMn_{1-x}Se$ for $x \leq 0.5$ possess the *wurtzite* structure.) In addition, we studied CVD-grown free-standing films of CdS, which have the wurtzite structure, using radiation polarized parallel and perpendicular to the optic axis lying in the plane of the film. We also present the results on a ~ 1 μm-thick epilayer of cubic 3C-SiC on a Si (100) substrate grown by CVD. Finally, we show the transmission spectra of MBE-grown GaAs and AlAs epilayers.

The transmission spectra were obtained with a BOMEM DA.8 rapid scanning Fourier transform infrared spectrometer,[14] capable of a maximum unapodized resolution of 0.0026 cm^{-1}, employing a high pressure Hg lamp as the source and a mylar beam-splitter. Typical spectra were recorded with 0.2–0.5 cm^{-1} resolution and 100 coadditions. A 4.2 K composite Si bolometer[15] with a long-pass cold filter and cone optics was used as a detector. The samples were cooled to 5K in a Janis Supervaritemp 10DT optical cryostat[16] with polypropylene windows. The angle between the incident beam and the normal to the surface of the thin film (θ_i) was adjusted by rotating the sample rod, which could be set to within $\sim 1°$ of the desired angle.

For the films grown on a substrate, the back of the substrate was polished and a wedge introduced deliberately in order to avoid *channeling* in the spectrum. This was accomplished by grinding with carborundum grit followed by 3-μm diamond paste and polishing with 0.05-μm alumina in distilled water. The orientation of the uniaxial crystals was determined by the Laue back reflection method. A wire grid polarizer[17] on a polyethylene substrate was used in the measurements where polarized radiation was necessary.

III. THEORETICAL CONSIDERATIONS

Consider a free-standing film of thickness d and dielectric function $\epsilon = n^2(\omega)$. An electromagnetic wave of frequency ω is incident on the film at an angle θ_i, with the electric field polarized either perpendicular (s,TE) or parallel (p,TM) to the plane of incidence. The ratio of the transmitted (t) and reflected (r) to incident (i) elec-

tric and magnetic fields can be calculated by applying the appropriate boundary conditions. For TE waves the ratios are

$$\frac{E_t}{E_i} = \left[\cos\kappa d - i\left(\frac{\kappa^2 + k^2}{2\kappa k}\right)\sin\kappa d\right]^{-1} \quad (1)$$

and

$$\frac{E_r}{E_i} = i\left(\frac{\kappa^2 - k^2}{2\kappa k}\right) \times \sin\kappa d\left[\cos\kappa d - i\left(\frac{\kappa^2 + k^2}{2\kappa k}\right)\sin\kappa d\right]^{-1}, \quad (2)$$

while for TM waves

$$\frac{B_t}{B_i} = \left[\cos\kappa d - i\left(\frac{\kappa^2 + n^4k^2}{2n^2\kappa k}\right)\sin\kappa d\right]^{-1} \quad (3)$$

and

$$\frac{B_r}{B_i} = i\left(\frac{\kappa^2 - n^4k^2}{2n^2\kappa k}\right) \times \sin\kappa d\left[\cos\kappa d - i\left(\frac{\kappa^2 + n^4k^2}{2n^2\kappa k}\right)\sin\kappa d\right]^{-1}. \quad (4)$$

Here $k = (\omega/c)\cos\theta_i$ and $\kappa = (\omega/c)[n^2 - \sin^2\theta_i]^{1/2}$. The fractional transmission (T) and reflection (R) are the magnitude squared of these quantities. These expressions are general and apply to films of any thickness.

In a polar *thin* film ($\omega/c \gg d$) there exist two *uniform* normal modes of vibration. They are deduced simply from the equations of motion of the positive and negative ions and noting that a depolarizing electric field equal to $-4\pi\vec{P}$ develops when the polarization $\vec{P}$ is normal to the plane of the film and zero when it lies in the plane. These normal modes have the LO and TO frequencies, respectively. Since the particle motion in the mode of frequency $\omega_{\rm LO}$ is perpendicular to the plane of the film, it cannot be excited by a TE wave. However, it can be excited by a TM wave incident obliquely on the film because the electric field then has a component in the direction of the particle motion.

In order to obtain meaningful results in the region of the normal mode frequencies, it is necessary to use a frequency-dependent dielectric function. For polar semiconductors,

$$n^2(\omega) = \epsilon_\infty + \frac{\epsilon_0 - \epsilon_\infty}{1 - (\omega/\omega_{\rm TO})^2 - i\gamma(\omega/\omega_{\rm TO})}, \quad (5)$$

and in the presence of free carriers,

$$n^2(\omega) = \epsilon_\infty + \frac{\epsilon_0 - \epsilon_\infty}{1 - (\omega/\omega_{\rm TO})^2 - i\gamma(\omega/\omega_{\rm TO})} - \frac{\epsilon_\infty}{(\omega/\omega_p)^2 + i\gamma_p(\omega/\omega_p)}, \quad (6)$$

where γ_p is the plasma damping coefficient and the plasma frequency $\omega_p = (4\pi Ne^2/m^*\epsilon_\infty)^{1/2}$, with N being the free carrier concentration and m^* the effective mass. Figure 1 shows the calculated transmission for (a) normal incidence, (b) $\theta_i = 45°$ and s polarization, and (c) $\theta_i = 45°$ and p polarization, using Eq. (5) in Eqs. (1)–(4) and values appropriate[18] for a 2-μm-thick film of ZnTe with $\gamma = 10^{-4}$: $\omega_{\rm TO} = 181$ cm^{-1}, $\epsilon_0 = 9.67$, and $\epsilon_\infty = 7.28$. It is seen that a transmission minimum appears at $\omega_{\rm TO}$ for all three cases while only for p polarization is there a minimum at $\omega_{\rm LO}$, as expected from the above description of the normal modes.

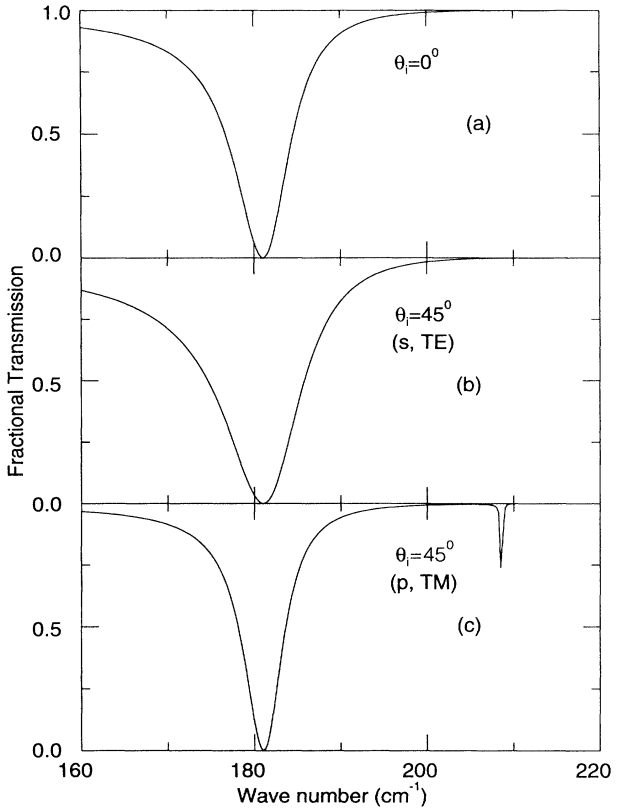

FIG. 1. Calculated fractional transmission of a thin ZnTe film in vacuum. (a) $\theta_i = 0°$, Eqs. (1) or (3); (b) $\theta_i = 45°$, s polarization, Eq. (1); (c) $\theta_i = 45°$, p polarization, Eq. (3). The parameters are listed in Sec. III.

A composite structure consisting of several layers, each with its characteristic optical constants, gives rise to transmission and reflection coefficients which are calculated by a successive application of the boundary conditions at each interface.[19] Each layer is charaterized by a 2×2 matrix relating the tangential components of the electric and magnetic fields at the entry side to those at the exit side of the layer. For the jth layer, this matrix has components $M_{11} = M_{22} = \cos\kappa_j d_j$, $M_{12} = -(i\omega/c\kappa_j)\sin\kappa_j d_j$ and $M_{21} = -(ic\kappa_j/\omega)\sin\kappa_j d_j$ for the TE mode. For the TM mode M_{11} and M_{22} are the same as for the TE mode, but $M_{12} = (i\omega n_j^2/c\kappa_j)\sin\kappa_j d_j$ and $M_{21} = (ic\kappa_j/\omega n_j^2)\sin\kappa_j d_j$. Here $\kappa_j = (\omega/c)[n_j^2 - \sin^2\theta_i]^{1/2}$, where n_j is the index of refraction of the jth layer and d_j is its thickness. An entire N layer stack is then described by the matrix

$$M_T = M_1 M_2 \cdots M_N = \begin{pmatrix} A & B \\ C & D \end{pmatrix}, \tag{7}$$

where M_1 is the matrix characterizing the layer on which the radiation is incident. For the stack the amplitude ratios are given by

$$t = \frac{2}{A + D \pm B\cos\theta_i \pm (C/\cos\theta_i)} \tag{8}$$

and

$$r = \frac{A - D \pm B\cos\theta_i \mp (C/\cos\theta_i)}{A + D \pm B\cos\theta_i \pm (C/\cos\theta_i)} \tag{9}$$

and, as before, $T = t^*t$ and $R = r^*r$. In these expressions, when the sign is ambiguous, the upper (lower) sign corresponds to the TE (TM) mode; t is (E_t/E_i) for the TE mode and (B_t/B_i) for the TM mode with a similar definition for the reflected amplitudes. Using this technique it is possible to calculate the transmission and reflection spectra for structures with many layers without difficulty and compare them with those obtained experimentally.

As previously noted, Eqs. (1)–(4) are general and apply to films of any thickness and it is of interest to study the effect of the thickness of the film on its transmission. Figure 2 shows simulated spectra for films of ZnTe of various thicknesses for TM radiation at oblique incidence. A progression from the two transmission dips, at ω_{TO} and ω_{LO}, in the 1-μm-thick film, to a broad region of zero transmission covering almost the entire reststrahlen band for the 100-μm-thick film is observed. In addition, interference fringes are seen, in the two thicker films, just below the TO frequency. This results from the rapid increase in the dielectric function before reaching the pole at ω_{TO}.

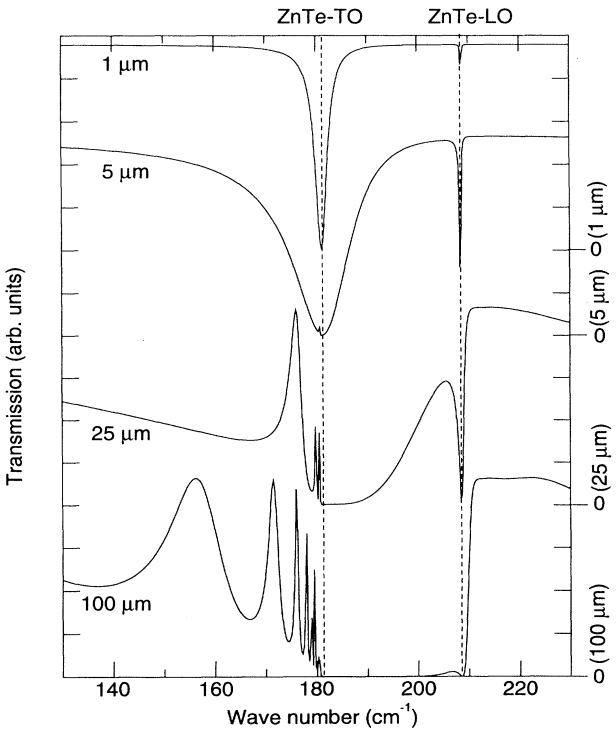

FIG. 2. Evolution of the transmission of ZnTe films for increasing thicknesses. (The parameters are listed in Sec. III.) Each spectrum is for $\theta_i = 45°$ and p polarization. For clarity, spectra for films of different thickness have been vertically displaced with the zero transmission being shown for each on the right-hand side.

IV. RESULTS AND DISCUSSION

The infrared transmission of a 1-μm zinc-blende MnTe epilayer, grown by MBE on a (001) GaAs substrate with a 2-μm ZnTe buffer, is shown in Fig. 3(a) for normal incidence, Fig. 3(b) for $\theta_i = 45°$, s polarization, and Fig. 3(c) for $\theta_i = 45°$, p polarization. As predicted by theory, only the TO phonons of the ZnTe buffer and of the MnTe

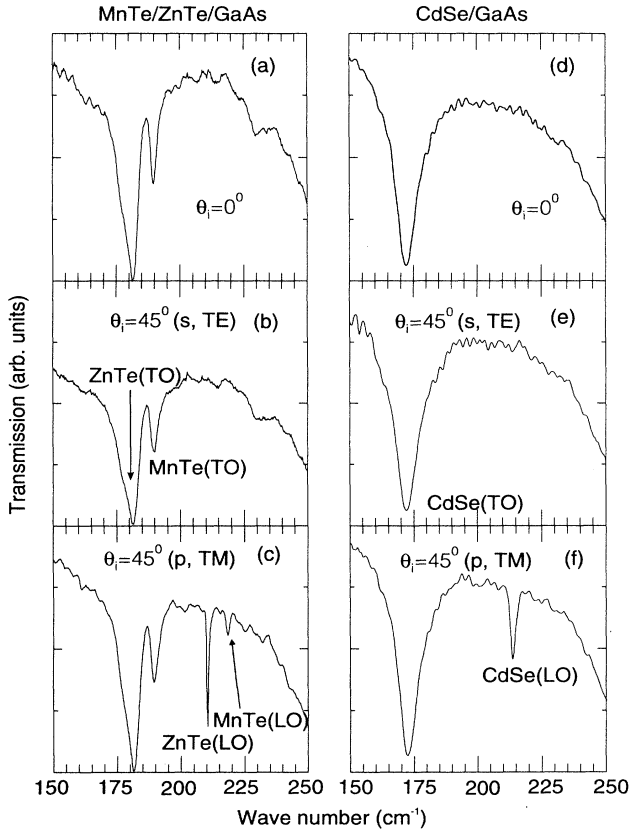

FIG. 3. Infrared transmission spectra of zinc-blende MnTe epilayer on a GaAs substrate with a ZnTe buffer layer for (a) $\theta_i = 0°$, (b) $\theta_i = 45°$, s polarization, and (c) $\theta_i = 45°$, p polarization and of a zinc-blende CdSe epilayer on a GaAs substrate for (d) $\theta_i = 0°$, (e) $\theta_i = 45°$, s polarization, and (f) $\theta_i = 45°$, p polarization. All the spectra were recorded at 5 K with a resolution of 0.5 cm^{-1}. The signatures associated with the LO phonons are observed only in (c) and (f) as expected from the theory.

epilayer, labeled ZnTe(TO) and MnTe(TO), respectively, are observed as transmission minima in the geometries employed in Figs. 3(a) and 3(b), whereas both TO and LO phonons of the buffer and of the epilayer are observed as transmission minima in the geometry used in Fig. 3(c). The positions of the ZnTe TO and LO phonons at 181.5 cm^{-1} and 210.4 cm^{-1}, respectively, are in good agreement with the Raman lines[20] at 181 cm^{-1} and 210 cm^{-1} and satisfy the LST relation with $\epsilon_0 = 9.67$ and $\epsilon_\infty = 7.28$. The MnTe TO and LO phonon positions of 189.7 cm^{-1} and 218.5 cm^{-1}, respectively, represent unstrained values of these phonon frequencies because the thickness of the MnTe epilayer has exceeded the pseudomorphic limit for the growth of MnTe on ZnTe. In addition, they are consistent with the TO (185 cm^{-1}) and LO (216 cm^{-1}) frequencies of zinc-blende MnTe deduced from the Raman data for bulk $Cd_{1-x}Mn_xTe$ and $Zn_{1-y}Mn_yTe$ by extrapolating to $x = 1$ and $y = 1$ using the modified random element isodisplacement (MREI) model,[21] the Raman values[20] being obtained at 80 K. However, the present values of MnTe LO and TO frequencies represent a *direct* experimental determination. Pelekanos *et al* [22] have observed the MnTe LO at 205 cm^{-1} in the Raman spectrum of a CdTe/MnTe single quantum well, the decrease from the 216 cm^{-1} value being attributed to the strain associated with the lattice mismatch between CdTe and MnTe. The rapid drop in transmission in Figs. 3(a)–3(c) at higher frequencies is produced by the onset of the reststrahlen of the GaAs substrate ($\omega_{TO} = 271.6$ cm^{-1}).

CdSe grown by MBE on (001) zinc-blende GaAs also possesses the zinc-blende structure and Figs. 3(d), 3(e), and 3(f) show the infrared transmission of such a CdSe epilayer for $\theta_i = 0°$ and unpolarized radiation, $\theta_i = 45°$ and s polarization, and $\theta_i = 45°$ and p polarization, respectively. As in the case of the MnTe epilayer, only the CdSe TO phonon is observed in Figs. 3(d) and 3(e), whereas both LO and TO phonons are observed in Fig. 3(f) with $\omega_{TO} = 171.9$ cm^{-1} and $\omega_{LO} = 213.2$ cm^{-1}, which again represent unstrained values. The ω_{LO} is in good agreement with the Raman value of 212.6 cm^{-1} measured in the same epilayer.[23] The present direct measurement of ω_{TO}, forbidden in Raman backscattering along [001], confirms the ω_{TO} deduced using the MREI model in Ref. 23.

Unlike the MBE-grown epilayers which adopt the structure of the underlying (001) zinc-blende GaAs substrate, CVD grown films of CdS possess the wurtzite structure of bulk CdS. In the specimens studied the optic axis ($\hat{c}$) was found to lie in the plane of the film. CdS belongs to the C_{6v}^4 space group and hence the zone-center optical phonons are classified according to the irreducible representations of C_{6v} as follows: one totally symmetric (A_1) infrared and Raman active, one doubly degenerate (E_1) infrared and Raman active, two doubly degenerate (E_2) Raman active, and two antisymmetric (B_1) *silent modes* inactive in both infrared and Raman. For phonon propagation $\mathbf{q} \perp \hat{c}$, the long range polarization splits the E_1 phonon into E_1(TO) and E_1(LO), whereas the A_1 phonon remains as A_1(TO). For $\mathbf{q} \parallel \hat{c}$, the E_1 phonon remains as E_1(TO), but the long range polarization field changes A_1(TO) to A_1(LO). In the Berreman experiment, noting that the vibrations in the plane of the film occur at ω_{TO}, whereas those perpendicular to the plane of the film occur at ω_{LO} due to the depolarizing surface charge, it is straightforward to deduce the infrared activity of the zone-center optical phonons for the different geometries permitted in the experiment as summarized in Table I. The infrared transmission spectra of a $\sim$ 25-μm-thick film of CdS for the geometries permitted when $\hat{c}$ lies in the plane of the film are shown in Fig. 4. Although the significant thickness of the film precluded the observation of a well defined transmission minimum at ω_{TO}, the simulations such as the one for ZnTe in Fig. 2 suggest that ω_{TO} is the frequency at the onset of zero transmission. The positions of the phonons identified according to the selection rules summarized in Table I are $\omega_{TO}(A_1)$=234 cm^{-1}, $\omega_{TO}(E_1)$=243 cm^{-1}, and $\omega_{LO}(E_1)$=307.1 cm^{-1}. The rapid oscillations just below ω_{TO} stem from the dramatic increase of the dielectric function as the frequency approaches its pole at ω_{TO}. The phonon frequencies reported here are in good

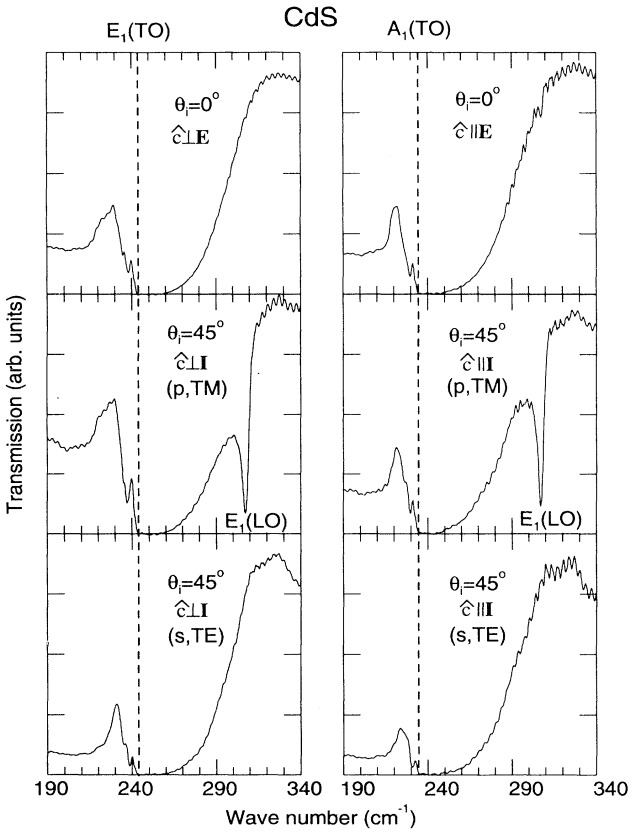

FIG. 4. Infrared transmission spectra of a ~25-μm-thick free-standing CdS film for the various geometries permitted when the optic axis lies in the plane of the film. $\hat{c} \perp \mathbf{I}$ and $\hat{c} \parallel \mathbf{I}$ refer to the geometries where $\hat{c}$, the optic axis is perpendicular and parallel to **I**, the plane of incidence, respectively. The appearance of the features labeled A_1(TO), E_1(TO), and E_1(LO) are consistent with their activity listed in Table I. The spectra were recorded at 5 K with a resolution of 0.5 cm^{-1}.

TABLE I. The infrared activity of the totally symmetric (A_1) and doubly degenerate (E_1) TO and LO phonons of a uniaxial crystal in the various geometries permitted in the Berreman experiment. $\hat{c} \parallel f$ and $\hat{c} \perp f$ refer to films in which the optic axis lies in the plane of the film or is perpendicular to it, respectively. $\hat{c} \parallel \mathbf{I}$ and $\hat{c} \perp \mathbf{I}$ refer to geometries in which the optic axis is in the plane of incidence or perpendicular to it, respectively.

	$\theta_i = 0$		$\theta_i \neq 0$, s polarization		$\theta_i \neq 0$, p polarization	
	$\mathbf{E} \parallel \hat{c}$	$\mathbf{E} \perp \hat{c}$	$\hat{c} \parallel \mathbf{I}$	$\hat{c} \perp \mathbf{I}$	$\hat{c} \parallel \mathbf{I}$	$\hat{c} \perp \mathbf{I}$
$\hat{c} \parallel f$	A_1(TO)	E_1(TO)	E_1(TO)	A_1(TO)	A_1(TO), E_1(LO)	E_1(TO), E_1(LO)
$\hat{c} \perp f$		E_1(TO)	E_1(TO)		E_1(TO), A_1(LO)	

agreement with those reported in the literature.[24] We note that as the film thickness increases, the onset of zero transmission occurs at frequencies lower than ω_{TO} and thus an accurate determination of ω_{TO} is not possible in such cases. The agreement of the ω_{TO} deduced from our measurement with those reported indicates that the films studied are not so thick as to preempt an accurate measurement of ω_{TO}. We also note that, in order to observe the A_1(LO) phonon using this technique, one requires a thin film with $\hat{c}$ perpendicular to the plane of the film.

The multimode behavior of II-VI ternaries and quaternaries has been extensively investigated using Raman spectroscopy[25] and the advent of nonequilibrium growth techniques has permitted the observation of phonons in compositions inaccessible in bulk growth. However, the geometry typically used in the Raman experiments on epilayers precludes the observation of the TO phonons whose behavior is indirectly inferred from the MREI model. We have studied the infrared transmission in a series of zinc-blende $Zn_{1-x}Cd_xSe$ and $Cd_{1-x}Mn_xSe$ epilayers on GaAs substrates and the phonon frequencies agree well with those reported.[26] Figure 5 illustrates the power of this technique, where a single transmission experiment at oblique incidence yielded the frequencies of the "CdSe-like" TO and LO as well as of the "MnSe-like" TO and LO phonons in $Cd_{0.60}Mn_{0.40}Se$ and $Cd_{0.50}Mn_{0.50}Se$ epilayers observed as transmission minima. The reason for the small intensity of the CdSe-like LO phonon is not clear.

As another example of the versatility of this technique, we have studied the transmission of a CVD grown layer of 3C-SiC on a (001) Si substrate. In the context of wide gap semiconductors and their optoelectronic applications, SiC is receiving increasing attention. Although SiC is a IV-IV semiconductor, the larger electropositivity of Si leads to a charge separation in the unit cell and consequently an LO-TO splitting of the zone-center optical mode. The charge separation is quantified by the effective charge (e^*/e), which has been reported by several workers[27] to be approximately 1. The infrared transmission spectra at normal (upper) and oblique (lower) incidence are shown in Fig. 6 and the signature associated with the LO phonon is clearly observed. The phonon frequencies are found to be ω_{TO} =795 cm^{-1} and ω_{LO} =972.2 cm^{-1}; they are close to the Raman shifts reported by Olego and Cardona.[28] Given the thickness of the SiC film used, ω_{TO} was deduced in the same manner as for the CdS film and hence somewhat underestimated.

The observation of both the ZnTe and MnTe phonons in the bilayer of Fig. 3 shows that this technique can be extended to multilayer systems such as semiconductor superlattices, in agreement with the results predicted by the matrix method described in Sec. III. Two effects that influence the positions of the observed phonons in superlattices are (1) a rigid displacement of the entire phonon dispersion induced by the strain associated with lattice mismatch between the constituents and (2) confinement of phonons in ultra-thin layers requiring them to have wave vectors $q=(2\pi/a)(m/n)$, where a is the

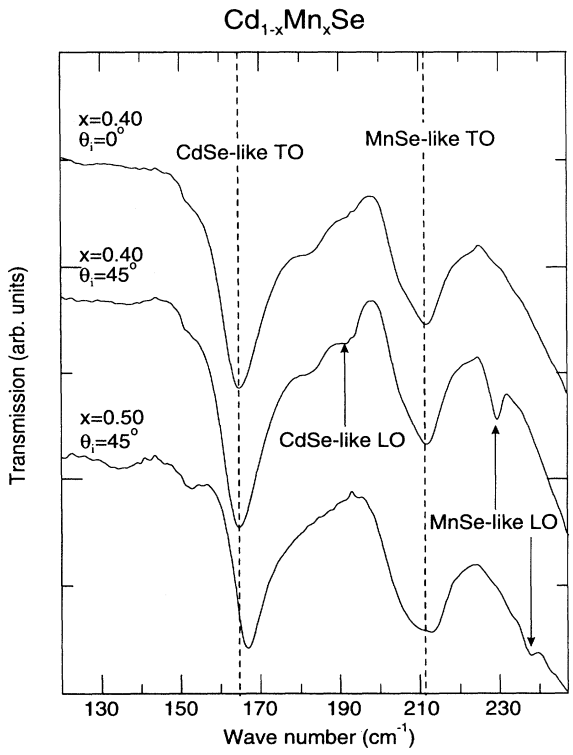

FIG. 5. Infrared transmission spectra of $Cd_{1-x}Mn_xSe$ epilayers on GaAs for $x = 0.40$ and $\theta_i = 0°$ (upper), $x = 0.40$ and $\theta_i = 45°$ (middle), and $x = 0.50$ and $\theta_i = 45°$ (lower), recorded at 5 K with a resolution of 0.5 cm^{-1}. The two-mode behavior of the ternary CdMnSe is clearly manifested as a shift in the CdSe-like and MnSe-like phonon frequencies in going from $x = 0.40$ to $x = 0.50$ and is entirely consistent with the results reported in Ref. 26. Incident light is unpolarized.

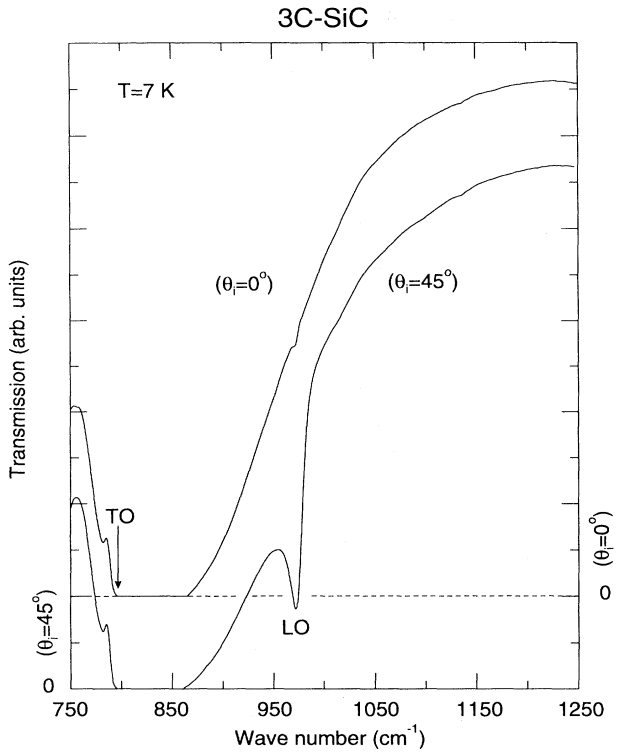

FIG. 6. Infrared transmission of a 3C-SiC epilayer grown by CVD on a Si substrate for normal (upper) and oblique (lower) incidence showing the onset of opacity close to ω_{TO} and the transmission minimum at ω_{LO}. Incident light is unpolarized.

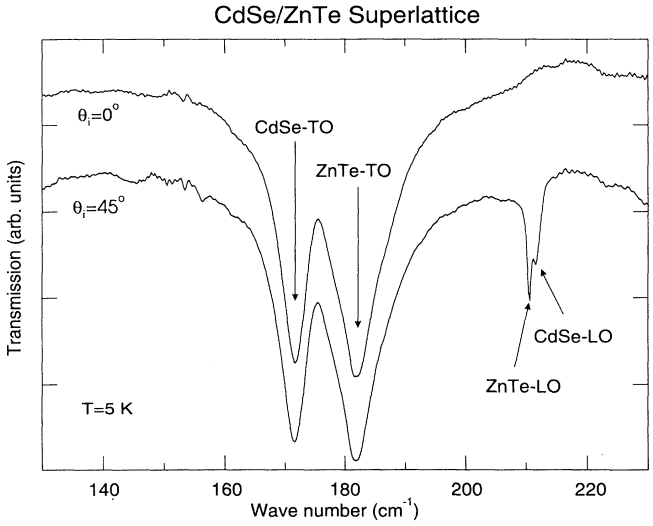

FIG. 7. Infrared transmission of a ZnTe/CdSe superlattice on GaAs for normal (upper) and oblique (lower) incidence, showing the strain shifted ZnTe and CdSe phonons. The superlattice consisted of 25 repeat periods of 90-Å ZnTe and 45-Å CdSe. Incident light is unpolarized.

lattice constant, n is the number of monolayers, and $m = 1, 2, 3, \ldots$ refers to the order of the phonon. Only the m-odd phonons are infrared active, their intensity being proportional to m^{-2}. The transmission spectra at normal and oblique incidence of the ZnTe/CdSe superlattice described in Sec. II are presented in Fig. 7. Signatures associated with the ZnTe and CdSe phonons are clearly observed as appropriately labeled minima. The small lattice mismatch of 0.76% between ZnTe and cubic CdSe is responsible for shifts of the phonon frequencies for ZnTe, ω_{TO} =181.7 cm^{-1} and ω_{LO} =210.4 cm^{-1}, and for CdSe, ω_{TO} =171.5 cm^{-1} and ω_{LO} =211.5 cm^{-1}, from their "strain-free" values of 181.5 cm^{-1} and 210.4 cm^{-1} (ZnTe) and 171.9 cm^{-1} and 213.2 cm^{-1} (CdSe). Since the layers of this superlattice are relatively thick, 45 Å (CdSe) and 90 Å (ZnTe), the frequency shift of the observed $m = 1$ phonons from their zone-center positions due to confinement is negligible. Orders greater than one are not experimentally observed in the infrared presumably due to lack of intensity.

We have studied many III-V semiconductor films and in Fig. 8(a) we present the results for two AlAs epilayers grown by MBE on GaAs substrates with GaAs cap layers. Although the thinner AlAs epilayer is only 200 Å thick, features due to both the TO and LO phonons are clearly observable thus showing the power of this technique to easily extract the zone-center phonon frequencies from very thin films. The LO and TO of AlAs, at 406.5 cm^{-1} and 364.0 cm^{-1} respectively, are not obscured by the reststrahlen of the GaAs substrate; these values are in excellent agreement with the Raman measurements.[29] When the AlAs epilayer is removed by a selective etch, the LO and TO of the 1.04-μm GaAs cap layer, floated onto a Si wafer, could be investigated; the Berreman tech-

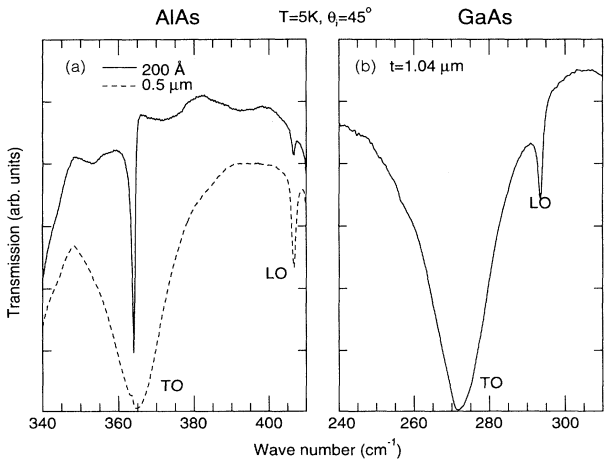

FIG. 8. (a) Infrared transmission spectra of a 200-Å and of a 0.5−μm AlAs epilayer grown by MBE on a GaAs substrate. Sharp signatures associated with the TO and LO phonons are clearly visible in spite of the very small thickness of one of the epilayers. (b) The infrared transmission of a 1.04-μm GaAs epilayer floated onto a Si substrate. Both (a) and (b) were measured with unpolarized radiation.

TABLE II. Comparison of the experimentally observed LO and TO phonon frequencies as measured by the Berreman technique with those by Raman scattering. All frequencies are in cm^{-1}.

	Berreman[a]			Raman		
Material	ω_{LO}	ω_{TO}	T (K)	ω_{LO}	ω_{TO}	T (K)
MnTe (cubic)	218.5	189.7	5	216.0	185.0[b]	80
ZnTe	210.4	181.5	5	210.0	181.0[b]	80
CdSe (cubic)	213.2	171.9	5	212.6	171.5[c]	5
CdS	307.1(E_1)	243±1(E_1)	5	306.9(E_1)	242.6(E_1)[d]	80
		234±1(A_1)	5	303.6(A_1)	234.7(A_1)[d]	80
SiC	972.2	795±2	7	973.0	796.5[e]	300
AlAs	406.5	364.0	5	404.9	363.5[f]	10
GaAs	293.4	271.6	5	296.4	273.1[g]	4.2
	294.2	272.4[h]	4.2			

[a]Present measurements. Unless otherwise indicated, their accuracy is ±0.1 cm^{-1}.
[b]Reference 20 (MREI fits to data on $Zn_{1-x}Mn_xTe$).
[c]Reference 23 (while ω_{TO}'s are from MREI fits to data on $Cd_{1-x}Mn_xSe$ and $Cd_{1-x}Zn_xSe$, ω_{LO} was observed directly for cubic CdSe).
[d]Reference 24.
[e]Reference 28.
[f]Reference 29.
[g]See A. Mooradian and G. B. Wright (Ref. 4).
[h]Reference 6. Note that these authors studied epitaxial GaAs grown on intrinsic Ge.

nique then yielded LO and TO frequencies of GaAs and Fig. 8(b) displays a typical spectrum with $\omega_{LO} = 293.4$ cm^{-1} and $\omega_{TO} = 271.6$ cm^{-1}.

In Table II we compare the data based on the Berreman technique with the Raman measurements available in the literature. It should be noted that the present values of ω_{LO} and ω_{TO} for cubic MnTe and ω_{TO} for cubic CdSe represent *direct* measurements of the frequencies of these modes.

V. CONCLUDING REMARKS

We have studied a wide variety of thin semiconductor films using infrared transmission at normal and oblique incidence, observing signatures at both ω_{TO} and ω_{LO}. We have also presented theoretical considerations for single and multiple layer thin films which fully account for the experimental results. It is important to judiciously choose thin film-substrate combinations such that the reststrahlen band of the substrate does not obscure the observation of the phonons of the thin film in transmission. However, in such cases the Berreman technique can be used in the reflection geometry.

In the case of thin films with wurtzite structure, the infrared active phonons may be polarized either parallel or perpendicular to the optic axis, offering many different geometries in which the Berreman experiment can be performed. Our results for CdS thin films with their optic axis in the plane of the film are in agreement with the theoretically predicted infrared activity of the A_1(TO), E_1(TO), and E_1(LO) phonons accessible in this geometry; with the optic axis normal to the film it would be possible to observe the A_1(LO) phonon also.

As is well known, the polar modes of the two alternating constituents in a superlattice may be "confined" to their respective layers. Using Raman spectroscopy, the evidence for such confinement in III-V superlattices has been reported by Sood *et al.*[30] and in II-VI superlattices by Suh *et al.*[31] and Oh *et al.*[32] The Berreman technique can now be profitably applied to discover similar effects in *both* ω_{TO} and ω_{LO}. Our preliminary measurements on $(CdTe)_n/(ZnTe)_n$ short period superlattices show evidence of such effects.[33] It should be noted that using resonant Raman scattering many orders of confined LO phonons can be observed, allowing a mapping of the LO phonon dispersion well into the Brillioun zone from studies on a single short period superlattice. However, only the first-order confined TO and LO phonons can be detected in the infrared with observable intensity, thus requiring several superlattice samples with different periods to achieve such a mappping of the TO and LO dispersion curves.

The collective oscillation of an electron gas in a metal—the longitudinal plasmon—is analogous to the LO lattice vibrations discussed in this paper and indeed has been directly observed in silver films by McAlister and Stern[34] using the Berreman effect. The dipolar plasmon in polar liquids predicted by Lobo, Robinson, and Rodriguez[35] was also experimentally demonstrated by Ascarelli[36] in the same manner in liquid nitromethane and nitromethane-CCl_4 solutions.

A very interesting problem that can be addressed with this technique is the coupled plasmon-phonon modes in doped semiconductors.[37] The accuracy with which the coupled mode frequencies could be measured would permit a precise determination of the effective mass dependence on carrier concentration, temperature, and alloy composition. We are currently pursuing such a study in n-$Al_{1-x}Ga_xAs$.

ACKNOWLEDGMENTS

The authors acknowledge support from the National Science Foundation: MRG Grant No. DMR 92-21390 (A.K.R., S.R., and J.K.F.); Grant No. DMR 93-03186 (A.K.R. and S.R.); and MRSEC Grant No. DMR 94-00415 (A.K.R. and M.R.M.). They are indebted to Dr. Donald C. Reynolds, Wright State University, for the free-standing, CVD grown CdS platelets.

[1] H. Rubens and E. F. Nichols, Weid. Ann. **60**, 418 (1897).
[2] M. Born and K. Huang, *Dynamical Theory of Crystal Lattices* (Oxford University Press, Oxford, England, 1968).
[3] R. B. Barnes and M. Czerny, Z. Phys. **72**, 447 (1931).
[4] L. Couture-Mathieu and J. P. Mathieu, C.R. Acad. Sci. **236**, 371 (1953); A. Mooradian and G. B. Wright, Solid State Commun. **4**, 431 (1966); W. G. Nilsen, Phys. Rev. **182**, 838 (1969).
[5] D. W. Berreman, Phys. Rev. **130**, 2193 (1963).
[6] S. Iwasa, I. Balslev, and E. Burstein, in *Proceedings of the Seventh International Conference on the Physics of Semiconductors*, edited by M. Hulin (Dunod, Paris, 1964), pp. 1077–1083.
[7] I. Richman, J. Chem. Phys. **41**, 2836 (1964).
[8] G. L. Bottger and A. L. Geddes, J. Chem. Phys. **46**, 3000 (1967).
[9] S. Iwasa, Ph.D. dissertation, University of Pennsylvania, 1966.
[10] H. D. Riccius, J. Appl. Phys. **39**, 4381 (1968).
[11] F. Proix and M. Balkanski, Phys. Status Solidi **32**, 119 (1969).
[12] A preliminary account has been presented in M. D. Sciacca, A. J. Mayur, E. Oh, A. K. Ramdas, and S. Rodriguez, Solid State Commun. **88**, 711 (1993).
[13] N. Samarth, H. Lou, J. K. Furdyna, S. B. Qadri, Y. R. Lee, R. G. Alonso, E. K. Suh, A. K. Ramdas, and N. Otsuka, Surf. Sci. **228**, 226 (1990).
[14] BOMEM Inc., 450 St. Jean Baptiste, Quebec, Canada, G2E 5S5.
[15] Infrared Laboratories, Inc., 1808 E. 17th Street, Tucson, AZ 85719.
[16] Janis Research Company, Inc., 2 Jewel Drive, Wilmington, MA 01887-0896.
[17] Perkin-Elmer Co., Norwalk, CT, Model 186-0082.
[18] *Semiconductors Other than Group IV Elements and III-V Compounds*, edited by O. Madelung (Springer-Verlag, Heidelberg, 1992), p. 28.
[19] The discussion in this section parallels that in M. Born and E. Wolf, *Principles of Optics* (Pergamon, New York, 1980), pp. 51–70.
[20] D. L. Peterson, A. Petrou, W. Giriat, A. K. Ramdas, and S. Rodriguez, Phys. Rev. B **33**, 1160 (1986).
[21] See, for example, L. Genzel, T. P. Martin, and C. H. Perry, Phys. Status Solidi B **62**, 83 (1974).
[22] N. Pelekanos, Q. Fu, J. Ding, W. Wałecki, A. V. Nurmikko, S. M. Durbin, J. Han, M. Kobayashi, and R. L. Gunshor, Phys. Rev. B **41**, 9966 (1990).
[23] R. G. Alonso, Y. R. Lee, E. Oh, A. K. Ramdas, H. Luo, N. Samarth, J. K. Furdyna, and H. Pascher, Phys. Rev. B **43**, 9610 (1991).
[24] R. J. Briggs and A. K. Ramdas, Phys. Rev. B **13**, 5518 (1976).
[25] E. Oh, R. G. Alonso, I. Miotkowski, and A. K. Ramdas, Phys. Rev. B **45**, 10 934 (1992).
[26] R. G. Alonso, E.-K. Suh, A. K. Ramdas, N. Samarth, H. Luo, and J. K. Furdyna, Phys. Rev. B **40**, 3720 (1989).
[27] E. Burstein and P. H. Egli, in *Advances in Electronics and Electron Physics*, edited by L. Marton (Academic, New York, 1955), Vol. 7, p. 1; W. G. Spitzer, D. Kleinman, and D. Walsh, Phys. Rev. **113**, 127 (1959).
[28] D. Olego and M. Cardona, Phys. Rev. B **25**, 1151 (1982).
[29] A. Onton, in *The Proceedings of the Tenth International Conference on the Physics of Semiconductors*, edited by S. P. Keller, J. C. Hensel, and F. Stern (USAEC Division of Technical Information Extension, Oak Ridge, TN, 1970), p. 107.
[30] A. K. Sood, J. Menéndez, M. Cardona, and K. Ploog, Phys. Rev. Lett. **54**, 2111 (1985).
[31] E.-K. Suh, D. U. Bartholomew, A. K. Ramdas, S. Rodriguez, S. Venugopalan, L. A. Kolodziejski, and R. L. Gunshor, Phys. Rev. B **36**, 4316 (1987).
[32] E. Oh, A. K. Ramdas, T. Fromherz, W. Faschinger, G. Bauer, and H. Sitter, Phys. Rev. B **48**, 17 364 (1993).
[33] A. J. Mayur, M. D. Sciacca, R. Vogelgesang, E. Oh, A. K. Ramdas, H. Pascher, T. Fromherz, G. Bauer, W. Faschinger, and H. Sitter (unpublished).
[34] A. J. McAlister and E. A. Stern, Phys. Rev. **132**, 1599 (1963).
[35] R. Lobo, J. E. Robinson, and S. Rodriguez, J. Chem. Phys. **59**, 5992 (1973).
[36] G. Ascarelli, Chem. Phys. Lett. **39**, 23 (1976).
[37] A. Mooradian and G. B. Wright, Phys. Rev. Lett. **16**, 999 (1966); H. R. Chandrasekhar and A. K. Ramdas, Phys. Rev. B **21**, 1511 (1980).